Geophysical Research Letters®

Key Points:

- Microclimatic disparities between Equatorial-facing slopes (EFSs) and polar-facing slopes (PFSs) shape distinct vegetation dynamics
- Global study reveals EFSs greener in colder regions, while PFSs show stronger greening trends, reflecting changing climate limitations
- Montane ecosystems provide insights into climate-driven vegetation growth, indicating temperature and water play pivotal roles

Supporting Information:

Supporting Information may be found in the online version of this article.

Correspondence to:

G. Yin,
yingf@swjtu.edu.cn

Author Contributions:

Conceptualization: Gaofei Yin, Josep Peñuelas
Funding acquisition: Gaofei Yin, Josep Peñuelas
Methodology: Jiangliu Xie, Dujuan Ma
Project Administration: Gaofei Yin, Josep Peñuelas
Supervision: Josep Peñuelas
Visualization: Jiangliu Xie
Writing – original draft: Gaofei Yin
Writing – review & editing: Qiaoyun Xie, Aleixandre Verger, Adrià Descals, Iolanda Filella, Josep Peñuelas

Aspect Matters: Unraveling Microclimate Impacts on Mountain Greenness and Greening

Gaofei Yin[1,2,3] , **Jiangliu Xie[1]**, **Dujuan Ma[1]**, **Qiaoyun Xie[4]**, **Aleixandre Verger[2,3,5]** , **Adrià Descals[2,3]**, **Iolanda Filella[2,3]**, and **Josep Peñuelas[2,3]**

[1]Faculty of Geosciences and Environmental Engineering, Southwest Jiaotong University, Chengdu, China, [2]CREAF, Cerdanyola del Vallès, Barcelona, Spain, [3]CSIC, Global Ecology Unit CREAF-CSIC-UAB, Barcelona, Spain, [4]School of Engineering, The University of Western Australia, Perth, WA, Australia, [5]CIDE, CSIC-UV-GV, València, Spain

Abstract Mountains are vital ecosystems, yet predicting plant growth there is complex due to diverse microclimates on slopes. Equatorial-facing slopes (EFSs) are drier and warmer, and polar-facing slopes (PFSs) are wetter and colder, than their regional macroclimates. Analyzing Moderate Resolution Imaging Spectroradiometer normalized difference vegetation index from 2003 to 2021, we identified a clear geographic pattern of differences in greenness on the two opposite aspects: EFSs were greener than PFSs in cold areas and were browner in dry areas, mainly determined by the relative importance of limitations of temperature and water. PFSs had stronger greening trends than did EPSs, leading to a weakening difference in greenness between EPSs and PFSs in temperature-limited areas, and an intensifying difference in water-limited areas. This suggests the alleviation of temperature limitation and exacerbation of water limitation. Montane ecosystems constitute a "natural laboratory" for deepening our understanding of the temporal evolution of the climatic control of vegetation growth with a space-for-time substitution.

Plain Language Summary Mountains are essential for Earth's greenery, but understanding plant growth in these landscapes is complex due to varied microclimates on slopes. Some slopes are drier and warmer, while others are wetter and colder than the surrounding areas. These micro-habitats influence how plants respond to changing climates. Using satellite data from 2003 to 2021, we found that slopes facing the equator are greener in cold areas but browner in dry zones. Slopes facing the poles have stronger greening trends than equatorial slopes. Our research reveals how mountain plants adapt to local conditions, offering insights into how they might respond to climate changes. Mountains act as nature's laboratories, guiding us in understanding how temperature and water shape plant growth over time.

1. Introduction

Terrestrial vegetation sequesters about one third of all anthropogenic carbon emissions, which is a key mechanism mitigating climatic warming (Friedlingstein et al., 2022). Both modeling and observational studies have indicated vegetation greening at the global scale over the last four decades (Chen et al., 2019; Huang et al., 2018; Myneni et al., 1997; Nemani et al., 2003; Zhu et al., 2016). Whether this increase in vegetation activity will continue in the future, however, remains uncertain (Penuelas et al., 2017; Zhang et al., 2022). One of the key uncertainties in the prediction of future vegetation dynamics is our limited understanding of the climatic control of vegetation growth (Nemani et al., 2003; Seddon et al., 2016). Continuing global warming is mitigating temperature limitations, particularly at high latitudes and elevations, while water constraints are becoming more widespread (Jiao et al., 2021; Li et al., 2022; Piao et al., 2014; Yin et al., 2022; Zhang et al., 2022). Predictions of vegetation dynamics in mountainous areas are particularly uncertain, primarily because of the complexity and ambiguity associated with microclimates formed by mountain topography (Barnard et al., 2017; Dobrowski, 2011).

Besides the well-known elevational gradients of climatic factors and their influence on vegetation activity (Gao et al., 2019; Vandvik et al., 2018), slope aspect plays a major role in shaping vegetation growth in mountainous areas (Barnard et al., 2017; Bennie et al., 2008; Fekedulegn et al., 2003; Gong et al., 2008; Kumari et al., 2020; Singh, 2018). Slope aspect modulates incident solar radiation, which in turn alters the fluxes of energy and water between the atmosphere and the surface, creating unique local microclimates with different near-surface temperatures and soil-moisture concentrations (Bennie et al., 2008). These microclimates can deviate markedly from the regional climates. For instance, equatorial-facing slopes (EFSs) receive more solar radiation than

polar-facing slopes (PFSs), leading to drier and hotter conditions on EFSs and wetter, colder conditions on PFSs than the regional macroclimatic conditions (Kumari et al., 2020). These aspect-induced microclimates significantly influence vegetation activity and may regulate the response of vegetation to regional climate change. Many studies have reported greater greenness and productivity on PFSs than on EFSs (Fekedulegn et al., 2003; Murphy et al., 2020). However, most of these studies relied on field observations, resulting in limited spatial coverage and short temporal spans. Consequently, the spatial distribution and interannual variation of the greenness difference across aspects at global scale remain unclear, hindering our understanding of the future trajectory of global mountain vegetation with climate change.

Satellite-derived vegetation indices have been found widespread applications in monitoring spatiotemporal variations in vegetation activity (Kumari et al., 2020; Yin et al., 2020). Among these indices, the normalized difference vegetation index (NDVI) is a widely used metric specifically designed to assess vegetation activity. It calculates the absorption of solar radiation by chlorophyll in the red band and its scattering by mesophyll in the near-infrared band (Huete et al., 2002). NDVI is recognized as a robust proxy for evaluating green biomass, demonstrating notable resilience against confounding factors such as topography and sun-observer geometry (Chen et al., 2020; Huete et al., 2002; Shen et al., 2009).

The primary objective of this study was to investigate the spatiotemporal patterns of differences in greenness between EFSs and PFSs and to explore their climatic controls using Satellite-derived NDVI. EFSs and PFSs often replicate conditions typical of colder and wetter present climates and hotter and drier future climates, respectively (Zhang et al., 2022). They serve as a "natural laboratory" for enhancing our understanding of the climatic influence on vegetation growth through a space-for-time substitution approach.

2. Materials and Methods

2.1. Data Sets

We used NDVI to represent vegetation greenness. NDVI is a vegetation index defined as the ratio of the difference between near-infrared and red reflectance to their sum. Specifically, we used data from the Moderate Resolution Imaging Spectroradiometer (MODIS) NDVI product (MOD13Q1) version 6.1, which are generated every 16 days at a spatial resolution of 250 m (Huete et al., 2002).

We generated global maps of slope and aspect using the 100 m ASTER Global Digital Elevation Model (AG100) data set (Fujisada et al., 2005). The slopes and aspects were then resampled to 250 m by averaging to match the data from the MODIS NDVI product.

Vegetation types were extracted following the International Geosphere-Biosphere Program (IGBP) based on the 500 m MODIS land-cover classification (MCD12Q1) (Friedl et al., 2002). The MCD12Q1 data was resampled to 250 m using the nearest-neighbor method to match the spatial resolution of the MODIS NDVI product.

We confined our analysis to mountainous areas, which were delineated using the Global Mountain Biodiversity Assessment (GMBA) Version 1.2 data set (Korner et al., 2017). GMBA identified an area as mountainous if the change in elevation between focal and neighboring cells was >200 m. Mountainous areas covered 26 million km^2, accounting for ~17.5% of the land area. The GMBA Version 1.2 data set is originally provided in vector format. For implementation purposes, we converted it into raster format with a spatial resolution of $0.5 \times 0.5°$.

The Climate Research Unit Time-Series version 4.06 (CRU TS4.06) data sets (Harris et al., 2020) with a spatial scale of 0.5° and a monthly temporal scale were used to calculate the mean annual temperature (MAT), cumulative annual precipitation and cumulative potential evapotranspiration.

2.2. Analysis

Global slopes and aspects were calculated using the AG100 data set. Values of 0 and 180° in the aspect map corresponded to north and south aspects, respectively. We identified pixels in the Northern Hemisphere as EFSs when their aspects were 135–225° and their slopes were >5°. Similarly, PFSs pixels corresponded to pixels with aspects of 315–360° or 0–45° and slopes >5°. The definitions of PFSs and EFSs pixels were opposite in aspect for the Southern and Northern Hemispheres.

The greenness difference index (GDI) was used to quantify the difference in vegetation activity between EFSs and PFSs. We used GDI for the peak of the growing season because it is the most representative time to identify
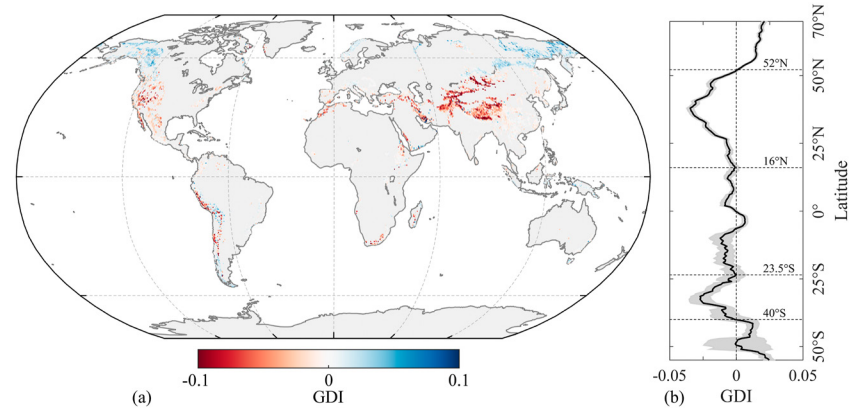
Figure 1. Spatial distribution of the greenness difference index (GDI) across equatorial-facing slopes and polar-facing slopes. (a) Average GDI during 2003–2021. (b) Latitudinal distribution of GDI; the black line and gray area represent average GDI and its standard deviation, respectively.

the interannual variability of productivity (Huang et al., 2018; Xia et al., 2015). The peak of the growing season was defined as the day with annual maximum NDVI. NDVI was averaged over the EFSs and PFSs for each $0.5 \times 0.5°$ grid cell, referred to as $NDVI_{EFS}$ and $NDVI_{PFS}$, respectively (see Figure S1 in Supporting Information S1 for examples of multiyear average cases). To ensure the reliability of the results, we selected MODIS observations with summary qualities in MOD13Q1 of 0 (indicating good data) and NDVIs >0.1 (to remove pixels without vegetation). Grid cells with <50 MODIS pixels containing neither PFSs nor EFSs were masked to obtain a robust result. GDI was then calculated as the normalized difference between $NDVI_{EFS}$ and $NDVI_{PFS}$, that is, $GDI = (NDVI_{EFS} - NDVI_{PFS})/(NDVI_{EFS} + NDVI_{PFS})$. GDI ranges between -1 and 1. A GDI <0 indicates that PFSs are greener than EFSs, and a GDI >0 indicates that EFSs are greener than PFSs.

Note that grid cells with GDIs, after controlling the quality as described above, are highly spatiotemporally variable, depending on the topography and image availability, which decreased the spatiotemporal homogeneity of GDI. For example, the grid for 0–45°N and <40°S were very few in 2001 and 2002, respectively, than in other years (Figure S2 in Supporting Information S1), so we limited our study to 2003–2021 to obtain robust results. Furthermore, the aspect-induced microclimates may also result in variations in vegetation types. Consequently, we conducted a comparative analysis of greenness and greening trends between PFSs and EFSs specifically for grassland, forest, and shrubland. We achieved this by extracting the respective NDVI values according to the MCD12Q1 product.

The trends reported in this paper were based on Theil–Sen slopes. This approach is insensitive to statistical outliers, because the median slope from a range of possible slopes is selected as the best fit (Fernandes & Leblanc, 2005). The significance of these slopes was determined based on Kendall's tau statistic from Mann–Kendall tests (Jiang et al., 2015).

3. Results

We first explored the spatial patterns of average GDI for 2003–2021 (Figure 1). GDI identified a clear latitudinal pattern. The EFSs were greener than the PFSs (GDI >0, blue) in most regions at high latitudes (>52°N and >40°S). The opposite pattern (GDI < 0, red) was mainly at intermediate latitudes (e.g., 16–52°N and 23.5–40°S). In the vicinity of the equator (23.5°S–16°N), there were no obvious differences in greenness observed between EFSs and PFSs (GDI ≈ 0).

To quantify the climatic control of the GDI distribution, we put GDI in a temperature-aridity space (Figure 2), in which temperature and aridity were respectively represented by MAT and the ratio of precipitation to potential evapotranspiration (P/PET), both averaged for 2003–2021. GDI was negative (greener PFSs than EFSs) in arid areas (P/PET ≤0.5), regardless of the regional temperature. The wetter microclimates of the PFSs in these areas could partially mitigate the limitation of water and promote the growth of vegetation. Humid areas (P/PET >0.5) had both positive and negative GDIs, depending on the regional temperature. In humid (P/PET >0.5) and cold (MAT < −2°C) areas where vegetation was mainly limited by low temperatures, the EFSs with warmer microhabitats favored vegetation growth, leading to positive GDIs. This positive effect attenuated or even reversed (negative GDIs) as temperature increased, because the higher evaporative demand may limit water on EFSs. In
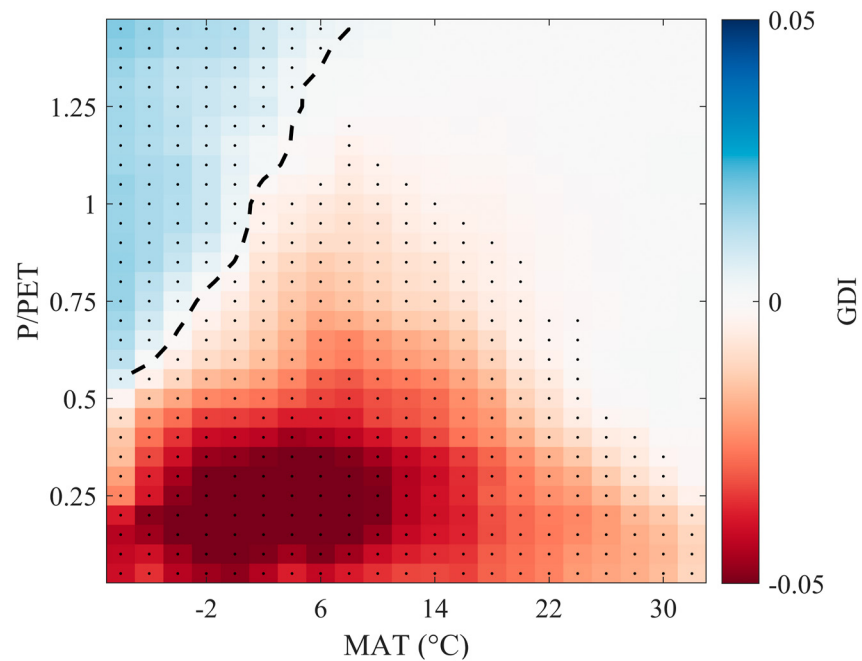
Figure 2. Greenness difference index (GDI) binned as a function of climatological mean annual temperature (MAT) and the ratio of precipitation to potential evapotranspiration (P/PET). Each bin is defined by 2°C intervals of MAT and 0.05 intervals of P/PET, based on macroclimatic conditions (calculated using the Climate Research Unit Time-Series version 4.06 data sets (Harris et al., 2020) averaged for 2003–2021). The dashed line delineates bins with positive and negative GDIs, representing areas limited by temperature and water, respectively. Dots represent bins with GDIs significantly different from zero (two-sided Student's t-test; $p < 0.05$).

summary, GDI identified the regional climatic control of vegetation growth, with areas limited by temperature and water (separated by the dashed line in Figure 2) having positive and negative GDIs, respectively.

Finally, we examined the temporal variation of the difference in vegetation on EFSs and PFSs for 2003–2021. Mountains had a widespread greening trend globally, and the greening trends of EFSs and PFSs were significant ($p < 0.1$) in 77.5% and 73.9% of the mountains, respectively (Figure S3 in Supporting Information S1). The greening trend was stronger for PFSs than EFSs: 0.0012 ± 0.0018 yr^{-1} versus 0.0011 ± 0.0018 yr^{-1} (mean $\pm$ standard deviation). The GDI trends were highly heterogeneous, with more grids with decreasing trends (Figure S4 in Supporting Information S1): the fractions of grids with significant ($p < 0.1$) decreasing and increasing trends were 16.5% and 10.0%, respectively. When averaged over the areas limited by temperature and water delineated from multiyear average positive and negative GDIs, respectively (see Figures 3a and 3b), NDVI increased significantly, with rates higher for PFSs than EFSs in both areas (see Figures 3c and 3d). GDI tended to decrease significantly in both the areas limited by temperature and water (see Figures 3e and 3f), consistent with the increasing trend of MAT (Figure S5 in Supporting Information S1) and the decreasing trend of P/PET (Figure S6 in Supporting Information S1).The areas limited by temperature and water had positive and negative GDIs, respectively, so the coincident decreasing trends in these two areas had opposite ecological consequences: the differences in greenness across the EFSs and PFSs weakened in areas limited by temperature and intensified in areas limited by water. We further investigated the vegetation type dependence of the greening trends of EFSs and PFSs (see Figures S7–S9 in Supporting Information S1). We noticed a consistent pattern across all vegetation types, albeit with varying degrees of magnitude. We also observed that forests are more frequently situated on PFSs, whereas shrubland and grassland tend to be predominantly located on EFSs (Figure S10 in Supporting Information S1).

4. Discussion and Conclusions

Different orientations of EFSs and PFSs generate contrasting microclimatic conditions that are decoupled from their regional macroclimates (Dobrowski, 2011). Specifically, PFSs are generally wetter and colder, and EFSs are generally drier and warmer, than their macroclimates (Kumari et al., 2020). We quantified the differences in
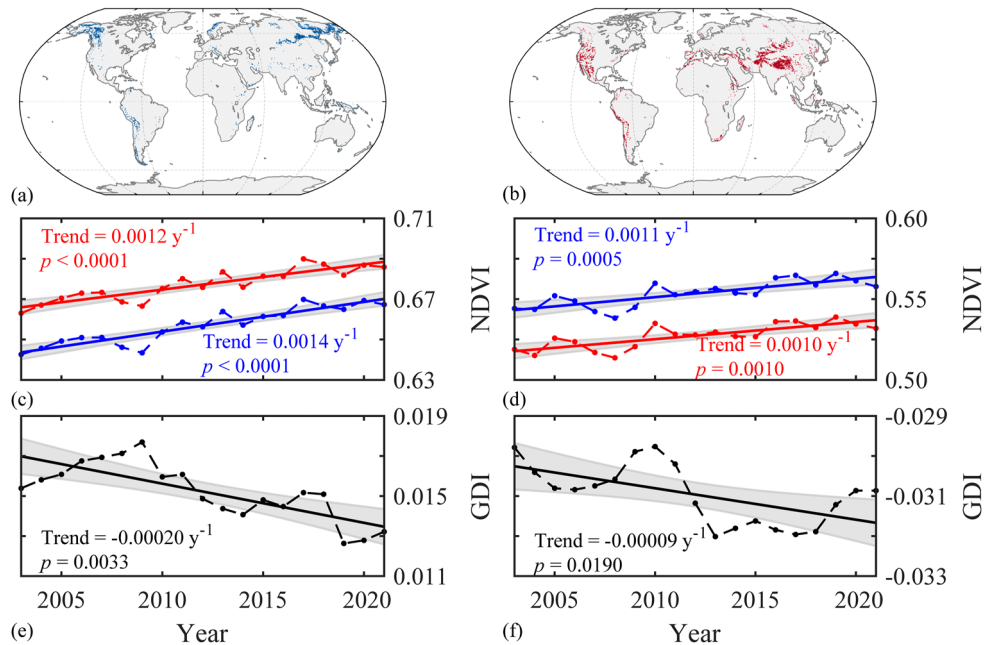
Figure 3. Temporal variations of NDVI and the greenness difference index (GDI) in areas limited by temperature (first column) and water (second column) for 2003–2021. Areas limited by temperature (blue shaded area in a) and water (red shaded area in b) are defined by positive and negative GDIs, respectively (Figure 1); (c) and (d) are NDVI and (e) and (f) are GDI for the two areas, respectively. NDVI for equatorial-facing slopes (red lines) and polar-facing slopes (blue lines) is shown in (c) and (d) to indicate their different trends under identical changes in regional climate.

greenness on EFSs and PFSs with GDI in each $0.5 \times 0.5°$ grid, and, for the first time, examined its spatiotemporal patterns at the global scale from 2003 to 2021. Our findings revealed a contrasting geographical pattern in GDI between areas limited by temperature and water. The majority of prior in-situ measurements have indicated that PFSs exhibit greater greenness and productivity compared to EFSs, primarily due to the underrepresentation of cold areas (Bale et al., 1998; Fekedulegn et al., 2003; Gong et al., 2008). We provide the first solid empirical evidence that the difference in greenness on EFSs and PFSs is determined by the relative importance of temperature and water limitations on regional vegetation growth. Negative GDI values (indicating PFSs are greener than EFSs) predominantly occur in regions constrained by water limitations, whereas positive GDI values (indicating EFSs are greener than PFSs) are prevalent in regions constrained by temperature. We also detected a widespread decreasing trend of GDI, indicating that the difference in greenness between EFSs and PFSs weakened in areas limited by temperature and intensified in areas limited by water.

We interpreted the geographical distribution of GDI using the relative importance of temperature and water limitation on regional vegetation growth, implying that the difference in greenness on EFSs and PFSs was mainly due to their contrasting microclimatic conditions. This hydrothermal difference could account for the global distribution of GDI (Figure 2), but local-scale GDI can be regulated by many other mechanisms. First, erosion and the weathering of soil are usually accelerated by high levels of insolation, so soil is less fertile and thinner on EFSs than PFSs (Hu et al., 2020; Poulos et al., 2012; Rech et al., 2001). Second, the dry and hot environments on EFSs increase the frequency of fire, intensifying plant mortality (Bradstock, 2010). Third, the active layer of permafrost soils at high latitudes is deeper on EFSs than PFSs (Dearborn et al., 2017). Finally, the steepness of slopes and diurnal movement of clouds may also affect the amount and diurnal cycle of solar radiation. The microclimates on different aspects are more complex than assumed in our study (Badano et al., 2005). Our main conclusions should therefore be interpreted with caution when transferring to local scale studies.

Some limitations of our analysis warrant attention. First, we used NDVI, which is insensitive to topographic distortion at the hectometeric resolution (Chen et al., 2020, 2022). However, the relatively coarse resolution of MODIS NDVI (250 m) may miss subtle terrain variations and hamper the collection of enough samples from each $0.5 \times 0.5°$ grid, potentially compromising the robustness of the results. Although finer spatial resolution satellite data, such as the 30-m Landsat observations, may alleviate this problem, it comes at the expense of

introducing other uncertainties such as the higher topographic effects on NDVI (Chen et al., 2020, 2022) and the lower revisiting frequency that would hamper identifying the peak of the growing season. Therefore, the 250-m MODIS NDVI is still likely the best data set we can currently use for a global-scale analysis. Prior to GDI computation, we rigorously employ quality control procedures, as detailed in the Materials and Methods section, to verify the presence of an adequate number of EFSs and PFSs pixels within each $0.5 \times 0.5°$ grid, thereby bolstering the reliability of our results. Second, the spatial resolutions of climatic data sets can also compromise the interpretation of our findings. We associated GDI with climatic factors at a spatial resolution of 0.5° due to the lack of fine-resolution climatic data sets that could characterize the differences of microclimates across aspects. Finally, dedicated field measurements on paired EFSs and PFSs at representative sites of global mountains are needed to fully characterize the mechanisms underlying the differences in vegetation on EFSs and PFSs.

Despite these limitations, our findings have several important implications. First, mountainous areas are foci of biodiversity, but the changing climate is threatening the maintenance of this biodiversity. The poleward shift across aspects is a complementary strategy of the upward elevational shift to reduce the loss of biodiversity, which can help plants disperse into favorable microclimates and buffer macroclimatic warming (Dobrowski, 2011). The poleward shift of species across aspects may affect species composition and reduce species diversity across aspects, thereby increasing the homogenization of vegetation across EFSs and PFSs (Feldmeier et al., 2020). We found that the vegetation was homogenized (reduced greenness difference across aspects) in areas limited by temperature rather than water, suggesting that poleward shifts may be more efficient in cold areas. Second, the evolution of the climatic control of vegetation is key for accurately predicting climate, but which is still highly debated (Descals et al., 2022; Yin et al., 2022; Zhang et al., 2021). The weakened difference in greenness on EFSs and PFSs in areas limited by temperature corroborates the alleviation of temperature limitation in cold areas (Keenan & Riley, 2018; Piao et al., 2014; Yin et al., 2022; Zhang et al., 2022). The intensified difference in greenness in areas limited by water provides new empirical evidence for the exacerbated limitation of water (Denissen et al., 2022; Jiao et al., 2021; Li et al., 2022; Zhang et al., 2021). It is worth noting that the temperature and water limitations indicated by GDI are relative. The exacerbated water limitation was in relation to temperature limitation, and it does not necessarily imply that the overall climatic limitation was intensified, as evidenced by the increased greenness in water-limited areas (Figure 3d). Finally, greening trends on vegetated surfaces have been widely reported, and we found that the greening trend was stronger on PFSs than EFSs (Figures 3c and 3d), suggesting that PFSs would profit more from the ongoing warming than would EFSs. Recent studies have reported that the availability of water regulates the response of vegetation to warming and that warming stimulates the growth of vegetation under wet conditions but depresses it under very dry conditions (Quan et al., 2019; Reich et al., 2018). EFSs and PFSs mirror dry and wet conditions, so the decreasing GDI trend supports the mechanism of water regulation of the response of vegetation to climatic warming (Quan et al., 2019; Reich et al., 2018). Our results indicate that gradients of EFS and PFS provide a "natural laboratory" for deepening our mechanistic understanding of the response of vegetation to continuous warming.

Data Availability Statement

All data used in this study are publicly available. The MOD13Q1 NDVI, MODIS land-cover (MCD12Q1) and ASTER DEM data are freely available on the Google Earth Engine platform, the GMBA data are available at https://www.gmba.unibe.ch/services/tools/mountain_inventory_v1, the Biome shapefile is available at https://www.sciencebase.gov/catalog/item/508fece8e4b0a1b43c29ca22 and the CRU TS4.06 data sets are available at https://crudata.uea.ac.uk/cru/data/hrg/.

References

Badano, E. I., Cavieres, L. A., Molina-Montenegro, M. A., & Quiroz, C. L. (2005). Slope aspect influences plant association patterns in the Mediterranean matorral of central Chile. *Journal of Arid Environments*, *62*(1), 93–108. https://doi.org/10.1016/j.jaridenv.2004.10.012

Bale, C. L., Williams, J. B., & Charley, J. L. (1998). The impact of aspect on forest structure and floristics in some Eastern Australian sites. *Forest Ecology and Management*, *110*(3), 363–377. https://doi.org/10.1016/s0378-1127(98)00300-4

Barnard, D. M., Barnard, H. R., & Molotch, N. P. (2017). Topoclimate effects on growing season length and montane conifer growth in complex terrain. *Environmental Research Letters*, *12*(6), 064003. https://doi.org/10.1088/1748-9326/aa6da8

Bennie, J., Huntley, B., Wiltshire, A., Hill, M. O., & Baxter, R. (2008). Slope, aspect and climate: Spatially explicit and implicit models of topographic microclimate in chalk grassland. *Ecological Modelling*, *216*(1), 47–59. https://doi.org/10.1016/j.ecolmodel.2008.04.010

Bradstock, R. A. (2010). A biogeographic model of fire regimes in Australia: Current and future implications. *Global Ecology and Biogeography*, *19*(2), 145–158. https://doi.org/10.1111/j.1466-8238.2009.00512.x

Chen, C., Park, T., Wang, X., Piao, S., Xu, B., Chaturvedi, R. K., et al. (2019). China and India lead in greening of the world through land-use management. *Nature Sustainability*, *2*(2), 122–129. https://doi.org/10.1038/s41893-019-0220-7

Chen, R., Yin, G., Zhao, W., Xu, B., Zeng, Y., Liu, G., & Verger, A. (2022). TCNIRv: Topographically corrected near-infrared reflectance of vegetation for tracking gross primary production over mountainous areas. *IEEE Transactions on Geoscience and Remote Sensing*, *60*, 1–10. https://doi.org/10.1109/tgrs.2022.3149655

Chen, R., Yin, G. F., Liu, G. X., Li, J., & Verger, A. (2020). Evaluation and normalization of topographic effects on vegetation indices. *Remote Sensing*, *12*(14), 2290. https://doi.org/10.3390/rs12142290

Dearborn, K. D., Danby, R. K., & Kikvidze, Z. (2017). Aspect and slope influence plant community composition more than elevation across forest-tundra ecotones in subarctic Canada. *Journal of Vegetation Science*, *28*(3), 595–604. https://doi.org/10.1111/jvs.12521

Denissen, J. M. C., Teuling, A. J., Pitman, A. J., Koirala, S., Migliavacca, M., Li, W., et al. (2022). Widespread shift from ecosystem energy to water limitation with climate change. *Nature Climate Change*, *12*(7), 677–684. https://doi.org/10.1038/s41558-022-01403-8

Descals, A., Verger, A., Yin, G., Filella, I., Fu, Y. H., Piao, S., et al. (2022). Radiation-constrained boundaries cause nonuniform responses of the carbon uptake phenology to climatic warming in the Northern Hemisphere. *Global Change Biology*, *29*(3), 719–730. https://doi.org/10.1111/gcb.16502

Dobrowski, S. Z. (2011). A climatic basis for microrefugia: The influence of terrain on climate. *Global Change Biology*, *17*(2), 1022–1035. https://doi.org/10.1111/j.1365-2486.2010.02263.x

Fekedulegn, D., Hicks, R. R., & Colbert, J. J. (2003). Influence of topographic aspect, precipitation and drought on radial growth of four major tree species in an Appalachian watershed. *Forest Ecology and Management*, *177*(1–3), 409–425. https://doi.org/10.1016/s0378-1127(02)00446-2

Feldmeier, S., Schmidt, B. R., Zimmermann, N. E., Veith, M., Ficetola, G. F., & Lötters, S. (2020). Shifting aspect or elevation? The climate change response of ectotherms in a complex mountain topography. *Diversity and Distributions*, *26*(11), 1483–1495. https://doi.org/10.1111/ddi.13146

Fernandes, R., & Leblanc, S. G. (2005). Parametric (modified least squares) and non-parametric (Theil-Sen) linear regressions for predicting biophysical parameters in the presence of measurement errors. *Remote Sensing of Environment*, *95*(3), 303–316. https://doi.org/10.1016/j.rse.2005.01.005

Friedl, M. A., McIver, D., Hodges, J., Zhang, X., Muchoney, D., Strahler, A., et al. (2002). Global land cover mapping from MODIS: Algorithms and early results. *Remote Sensing of Environment*, *83*(1–2), 287–302. https://doi.org/10.1016/s0034-4257(02)00078-0

Friedlingstein, P., O'Sullivan, M., Jones, M. W., Andrew, R. M., Gregor, L., Hauck, J., et al. (2022). Global carbon budget 2022. *Earth System Science Data*, *14*(11), 4811–4900. https://doi.org/10.5194/essd-14-4811-2022

Fujisada, H., Bailey, G. B., Kelly, G. G., Hara, S., & Abrams, M. J. (2005). ASTER DEM performance. *IEEE Transactions on Geoscience and Remote Sensing*, *43*(12), 2707–2714. https://doi.org/10.1109/tgrs.2005.847924

Gao, M., Piao, S., Chen, A., Yang, H., Liu, Q., Fu, Y. H., & Janssens, I. A. (2019). Divergent changes in the elevational gradient of vegetation activities over the last 30 years. *Nature Communications*, *10*(1), 2970. https://doi.org/10.1038/s41467-019-11035-w

Gong, X., Brueck, H., Giese, K., Zhang, L., Sattelmacher, B., & Lin, S. (2008). Slope aspect has effects on productivity and species composition of hilly grassland in the Xilin River Basin, Inner Mongolia, China. *Journal of Arid Environments*, *72*(4), 483–493. https://doi.org/10.1016/j.jaridenv.2007.07.001

Harris, I., Osborn, T. J., Jones, P., & Lister, D. (2020). Version 4 of the CRU TS monthly high-resolution gridded multivariate climate dataset. *Scientific Data*, *7*(1), 109. https://doi.org/10.1038/s41597-020-0453-3

Hu, G.-R., Li, X.-Y., & Yang, X.-F. (2020). The impact of micro-topography on the interplay of critical zone architecture and hydrological processes at the hillslope scale: Integrated geophysical and hydrological experiments on the Qinghai-Tibet Plateau. *Journal of Hydrology*, *583*, 124618. https://doi.org/10.1016/j.jhydrol.2020.124618

Huang, K., Xia, J., Wang, Y., Ahlström, A., Chen, J., Cook, R. B., et al. (2018). Enhanced peak growth of global vegetation and its key mechanisms. *Nature Ecology & Evolution*, *2*(12), 1897–1905. https://doi.org/10.1038/s41559-018-0714-0

Huete, A., Didan, K., Miura, T., Rodriguez, E., Gao, X., & Ferreira, L. (2002). Overview of the radiometric and biophysical performance of the MODIS vegetation indices. *Remote Sensing of Environment*, *83*(1–2), 195–213. https://doi.org/10.1016/s0034-4257(02)00096-2

Jiang, W., Yuan, L., Wang, W., Cao, R., Zhang, Y., & Shen, W. (2015). Spatio-temporal analysis of vegetation variation in the Yellow River Basin. *Ecological Indicators*, *51*, 117–126. https://doi.org/10.1016/j.ecolind.2014.07.031

Jiao, W., Wang, L., Smith, W. K., Chang, Q., Wang, H., & D'Odorico, P. (2021). Observed increasing water constraint on vegetation growth over the last three decades. *Nature Communications*, *12*(1), 3777. https://doi.org/10.1038/s41467-021-24016-9

Keenan, T. F., & Riley, W. J. (2018). Greening of the land surface in the world's cold regions consistent with recent warming. *Nature Climate Change*, *8*(9), 825–828. https://doi.org/10.1038/s41558-018-0258-y

Korner, C., Jetz, W., Paulsen, J., Payne, D., Rudmann-Maurer, K., & M. Spehn, E. (2017). A global inventory of mountains for bio-geographical applications. *Alpine Botany*, *127*(1), 1–15. https://doi.org/10.1007/s00035-016-0182-6

Kumari, N., Saco, P. M., Rodriguez, J. F., Johnstone, S. A., Srivastava, A., Chun, K. P., & Yetemen, O. (2020). The grass is not always greener on the other side: Seasonal reversal of vegetation greenness in aspect-driven semiarid ecosystems. *Geophysical Research Letters*, *47*(15), e2020GL088918. https://doi.org/10.1029/2020gl088918

Li, W., Migliavacca, M., Forkel, M., Denissen, J. M. C., Reichstein, M., Yang, H., et al. (2022). Widespread increasing vegetation sensitivity to soil moisture. *Nature Communications*, *13*(1), 3959. https://doi.org/10.1038/s41467-022-31667-9

Murphy, P. C., Knowles, J. F., Moore, D. J. P., Anchukaitis, K., Potts, D. L., & Barron-Gafford, G. A. (2020). Topography influences species-specific patterns of seasonal primary productivity in a semiarid montane forest. *Tree Physiology*, *40*(10), 1343–1354. https://doi.org/10.1093/treephys/tpaa083

Myneni, R. B., Keeling, C. D., Tucker, C. J., Asrar, G., & Nemani, R. R. (1997). Increased plant growth in the northern high latitudes from 1981 to 1991. *Nature*, *386*(6626), 698–702. https://doi.org/10.1038/386698a0

Nemani, R. R., Keeling, C. D., Hashimoto, H., Jolly, W. M., Piper, S. C., Tucker, C. J., et al. (2003). Climate-driven increases in global terrestrial net primary production from 1982 to 1999. *Science*, *300*(5625), 1560–1563. https://doi.org/10.1126/science.1082750

Penuelas, J., Ciais, P., Canadell, J. G., Janssens, I. A., Fernández-Martínez, M., Carnicer, J., et al. (2017). Shifting from a fertilization-dominated to a warming-dominated period. *Nature Ecology & Evolution*, *1*(10), 1438–1445. https://doi.org/10.1038/s41559-017-0274-8

Piao, S. L., Nan, H., Huntingford, C., Ciais, P., Friedlingstein, P., Sitch, S., et al. (2014). Evidence for a weakening relationship between inter-annual temperature variability and northern vegetation activity. *Nature Communications*, *5*(1), 5018. https://doi.org/10.1038/ncomms6018

Poulos, M. J., Pierce, J. L., Flores, A. N., & Benner, S. G. (2012). Hillslope asymmetry maps reveal widespread, multi-scale organization. *Geophysical Research Letters*, *39*(6), L06406. https://doi.org/10.1029/2012gl051283

Quan, Q., Tian, D., Luo, Y., Zhang, F., Crowther, T. W., Zhu, K., et al. (2019). Water scaling of ecosystem carbon cycle feedback to climate warming. *Science Advances*, *5*(8). https://doi.org/10.1126/sciadv.aav1131

Rech, J. A., Reeves, R. W., & Hendricks, D. M. (2001). The influence of slope aspect on soil weathering processes in the Springerville volcanic field, Arizona. *Catena*, *43*(1), 49–62. https://doi.org/10.1016/s0341-8162(00)00118-1

Reich, P. B., Sendall, K. M., Stefanski, A., Rich, R. L., Hobbie, S. E., & Montgomery, R. A. (2018). Effects of climate warming on photosynthesis in boreal tree species depend on soil moisture. *Nature*, *562*(7726), 263–267. https://doi.org/10.1038/s41586-018-0582-4

Seddon, A. W. R., Macias-Fauria, M., Long, P. R., Benz, D., & Willis, K. J. (2016). Sensitivity of global terrestrial ecosystems to climate variability. *Nature*, *531*(7593), 229–232. https://doi.org/10.1038/nature16986

Shen, M., Tang, Y., Klein, J., Zhang, P., Gu, S., Shimono, A., & Chen, J. (2009). Estimation of aboveground biomass using in situ hyperspectral measurements in five major grassland ecosystems on the Tibetan Plateau. *Journal of Plant Ecology*, *2*(1), 43. https://doi.org/10.1093/jpe/rtp002

Singh, S. (2018). Understanding the role of slope aspect in shaping the vegetation attributes and soil properties in Montane ecosystems. *Tropical Ecology*, *59*(3), 417–430.

Vandvik, V., Halbritter, A. H., & Telford, R. J. (2018). Greening up the mountain. *Proceedings of the National Academy of Sciences of the United States of America*, *115*(5), 833–835. https://doi.org/10.1073/pnas.1721285115

Xia, J., Niu, S., Ciais, P., Janssens, I. A., Chen, J., Ammann, C., et al. (2015). Joint control of terrestrial gross primary productivity by plant phenology and physiology. *Proceedings of the National Academy of Sciences of the United States of America*, *112*(9), 2788–2793. https://doi.org/10.1073/pnas.1413090112

Yin, G., Verger, A., Filella, I., Descals, A., & Peñuelas, J. (2020). Divergent estimates of forest photosynthetic phenology using structural and physiological vegetation indices. *Geophysical Research Letters*, *47*(18), e2020GL089167. https://doi.org/10.1029/2020gl089167

Yin, G. F., Verger, A., Descals, A., Filella, I., & Penuelas, J. (2022). Nonlinear thermal responses outweigh water limitation in the attenuated effect of climatic warming on photosynthesis in northern ecosystems. *Geophysical Research Letters*, *49*(16), e2022GL100096. https://doi.org/10.1029/2022gl100096

Zhang, A. Z., Jia, G. S., & Ustin, S. L. (2021). Water availability surpasses warmth in controlling global vegetation trends in recent decade: Revealed by satellite time series. *Environmental Research Letters*, *16*(7), 074028. https://doi.org/10.1088/1748-9326/ac0b68

Zhang, Y. C., Piao, S., Sun, Y., Rogers, B. M., Li, X., Lian, X., et al. (2022). Future reversal of warming-enhanced vegetation productivity in the Northern Hemisphere. *Nature Climate Change*, *12*(6), 581–586. https://doi.org/10.1038/s41558-022-01374-w

Zhu, Z., Piao, S., Myneni, R. B., Huang, M., Zeng, Z., Canadell, J. G., et al. (2016). Greening of the Earth and its drivers. *Nature Climate Change*, *6*(8), 791–795. https://doi.org/10.1038/nclimate3004